

# Electron Transfer Quenching and Electrochemiluminescence Comparative Studies of the Systems Containing *N*-Methylpyridinium Cations and Ru(2,2'-bipyridine)<sub>3</sub><sup>2+</sup> or Ru(1,10-phenanthroline)<sub>3</sub><sup>2+</sup> Complexes

Andrzej Kapturkiewicz\* and Pawel Szrebowaty

*Institute of Physical Chemistry, Polish Academy of Sciences, Kasprzaka 44/52, 01-224, Warsaw, Poland*

Gonzalo Angulo and Günter Grampp

*Institute of Physical and Theoretical Chemistry, Graz University of Technology, Technikerstrasse 4-1, A-8010 Graz, Austria*

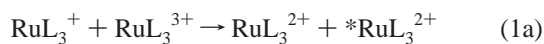
Received: July 31, 2001; In Final Form: November 29, 2001

Quenching of the luminescent state of tris(2,2'-bipyridine)ruthenium(II) and tris(1,10-phenanthroline)ruthenium(II) (Ru(bipy)<sub>3</sub><sup>2+</sup> and Ru(phen)<sub>3</sub><sup>2+</sup>) complexes by a series of pyridinium ions has been studied in 0.1M (C<sub>2</sub>H<sub>5</sub>)<sub>4</sub>-NPF<sub>6</sub> acetonitrile solutions. 4-Acetyl, 4-cyano, 4-carbomethoxy, and 4-carbamido-1-methylpyridium cations R<sup>+</sup> were employed as electron acceptor quenchers. The quenching rates were measured by using steady-state technique. Separation efficiencies of electron-transfer products were obtained by measurements of the transient absorbances of photogenerated *N*-methylpyridinium radicals R• using laser flash photolysis. The quenching rate constants and radical separation efficiencies were used for the calculation of the kinetic parameters for forward, reverse and back electron transfer. Opposite electron-transfer process, i.e., a generation of the excited states \*Ru(bipy)<sub>3</sub><sup>2+</sup> and \*Ru(phen)<sub>3</sub><sup>2+</sup> (in reactions Ru(bipy)<sub>3</sub><sup>3+</sup> + R• or Ru(phen)<sub>3</sub><sup>3+</sup> + R•, respectively), has been studied by means of the electrochemically generated chemiluminescence. Reaction schemes for both types of the electron transfer processes have been comparatively discussed concluding that the same set of the kinetic parameters may be successfully applied in quantitative description.

## 1. Introduction

Electrochemically generated chemiluminescence (ECL) can be defined as the generation of light-emitting species by means of homogeneous electron-transfer reactions between precursors in solution obtained as a consequence of heterogeneous (electrode) processes.<sup>1–5</sup> ECL can be observed for organic as well as inorganic compounds (e.g., transition metal complexes). The latter systems are often relatively simple from a mechanistic point of view, exhibiting two reaction pathways, i.e., the direct formation of emissive excited and ground states.<sup>6,7</sup>

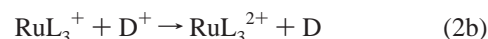
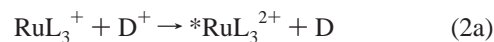
The widely studied examples (in ECL of transition metals complexes) are these concerning Ru(II) chelates (RuL<sub>3</sub><sup>2+</sup>)<sup>8–18</sup> with the Ru(bipy)<sub>3</sub><sup>2+</sup> (where bipy = 2,2'-bipyridine) in acetonitrile (ACN) solutions as the most noticeable example.<sup>8–13</sup> Reduced RuL<sub>3</sub><sup>+</sup> and oxidized RuL<sub>3</sub><sup>3+</sup> ions (obtained in one-electron reduction or oxidation of the parent RuL<sub>3</sub><sup>2+</sup>) undergo annihilation with the formation of the excited \*RuL<sub>3</sub><sup>2+</sup> species. When cyclic square potential wave between the reduction and oxidation potential is applied, the typical orange emission of \*RuL<sub>3</sub><sup>2+</sup>, which continues indefinitely if the potential stepping is maintained, may be observed. In the simplest approximation, the ECL mechanism can be formulated as follows:



The experimentally found high efficiencies of the excited \*RuL<sub>3</sub><sup>2+</sup> formation strongly suggest that the thermodynamically

favored reaction 1b, to form directly the ground-state product, is kinetically inhibited. For example, in the case of Ru(bipy)<sub>3</sub><sup>2+</sup> complex, the value of ECL efficiency  $\phi_{\text{ecl}}$  (in photons emitted per electrons transferred between the reduced Ru(bipy)<sub>3</sub><sup>+</sup> and the oxidized Ru(bipy)<sub>3</sub><sup>3+</sup>) was found to be strictly approaching (especially at low temperatures) the intrinsic luminescence quantum efficiency  $\phi_0$  of the emitter.<sup>13</sup> It was concluded that the formation efficiency of the excited \*Ru(bipy)<sub>3</sub><sup>2+</sup>,  $\phi_{\text{es}}$ , is near unity.  $\phi_{\text{ecl}} = 0.05$  for the Ru(bipy)<sub>3</sub><sup>2+</sup> systems at 25 °C is frequently used as the efficiency standard in the studies of other ECL processes. Other Ru(II) polypyridines, biquinolines, phenanthrolines, or bipyrazine complexes exhibit a similar behavior, but the appropriate  $\phi_{\text{ecl}}$  values are found to be strongly dependent on the ligand nature.<sup>14–18</sup> It arises from the differences in  $\phi_{\text{es}}$ , as well as in  $\phi_0$  values.

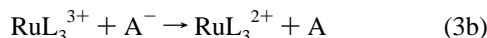
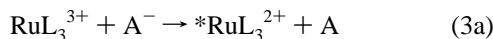
It is expected that sufficiently low energies of the excited \*RuL<sub>3</sub><sup>2+</sup> states allow also for the experimental observation of ECL phenomenon in mixed systems, i.e., in the reactions between RuL<sub>3</sub><sup>+</sup> and strong oxidant or between RuL<sub>3</sub><sup>3+</sup> and strong reductant (cf. ref 19). For example, electron-transfer (ET) reaction between stable radical cations D<sup>+</sup> (e.g., formed in the one-electron oxidation of aromatic amines D) and RuL<sub>3</sub><sup>+</sup> leads to a more or less efficient \*RuL<sub>3</sub><sup>2+</sup> generation:



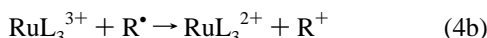
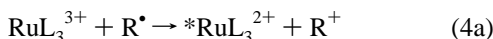
On the other hand, \*RuL<sub>3</sub><sup>2+</sup> generation may take place during ET reaction between RuL<sub>3</sub><sup>3+</sup> and stable radical anions A<sup>-</sup> (e.g.,

\* Corresponding author: e-mail akaptur@ichf.edu.pl.

formed in the one-electron reduction of aromatic nitrocompounds or quinones A):



In a similar way, neutral organic radicals  $\text{R}^\bullet$  (e.g., formed in the one-electron reduction of *N*-methylpyridinium cations  $\text{R}^+$ ) may be applied as reducing agent:



Excited-state generation of the organic co-reactants is not included in the reaction's pattern because their energies are usually high enough and their population is an energetically unfavorable process.

More detailed quantitative investigations of the above-mentioned processes have been recently performed in our laboratory for the mixed ECL systems involving  $\text{Ru}(\text{bipy})_3^{2+}$  complex. As it was expected (and reported previously for other ECL systems, e.g., ref 20), the functional dependence on the ET reaction exergonicity (i.e., free energy of the excited  $*\text{Ru}(\text{bipy})_3^{2+}$  population  $\Delta G_{\text{es}}$  as defined by eq 5) was found for both  $\text{Ru}(\text{bipy})_3^+ - \text{oxidant}$  and  $\text{Ru}(\text{bipy})_3^{3+} - \text{reductant}$  systems

$$\Delta G_{\text{es}} = -F(E_{\text{ox}} - E_{\text{red}}) + E_{\text{MLCT}} \quad (5)$$

where  $E_{\text{ox}}$  and  $E_{\text{red}}$  are the redox potentials of the ECL reaction partners,  $F$  is the Faraday constant, and  $E_{\text{MLCT}}$  is the energy of the excited  $*\text{RuL}_3^{2+}$ . It has been found that the experimentally determined  $\phi_{\text{ecl}}$  value increases and approaches a limiting value as  $\Delta G_{\text{es}}$  increases. However, the observed relationship between  $\phi_{\text{ecl}}$  and  $\Delta G_{\text{es}}$  has been found to be nonuniform. For the same  $\Delta G_{\text{es}}$ , the ECL efficiency depends on the organic reaction partners nature with the experimental points having a tendency to cluster (cf. Figure 1) around two (or three?) different curves (also after correction for the Coulombic interaction energies between the ET reactants or products). Similar results have been previously reported<sup>20</sup> for the ECL processes involving  $\text{Mo}_6\text{Cl}_{14}^{2-}$  ion ( $\text{Mo}_6\text{Cl}_{14}^{3-} + \text{D}^+$ ,  $\text{Mo}_6\text{Cl}_{14}^- + \text{A}^-$ , or  $\text{Mo}_6\text{Cl}_{14}^- + \text{R}^\bullet$  systems) and explained by the different ET distance in an activated complex, caused by the attractive or repulsive Coulombic interactions between oppositely or uniformly charged reactants.

The above explanation could not be applied in the case of the mixed ECL systems involving positively charged  $\text{Ru}(\text{bipy})_3^{2+}$  complex ( $\text{Ru}(\text{bipy})_3^+ + \text{D}^+$ ,  $\text{Ru}(\text{bipy})_3^{3+} + \text{A}^-$  or  $\text{Ru}(\text{bipy})_3^{3+} + \text{R}^\bullet$  systems) because it predicts an exactly opposite effect. It may be concluded that the simple explanation as proposed in ref 20 could not be general (or even wrong) and that the observed behavior may be a more general rule. In both cases (i.e., ECL processes involving ruthenium as well as molybdenum complexes), experimental values of  $\phi_{\text{ecl}}$  have a tendency to group into two classes corresponding (at the same  $\Delta G_{\text{es}}$ ) to relatively efficient or inefficient ECL systems. Appending of the particular organic reactant in a high-efficiency class (hec) or in a low-efficiency (lec) class is the same for both apparently different inorganic co-reactants.

More detailed and quantitative discussion of the  $\phi_{\text{ecl}}$  value for the given ECL system may be done in terms of an ET model for chemiluminescence,<sup>21</sup> first proposed by Marcus. Electron transfer between oxidized and reduced reactants leads competi-

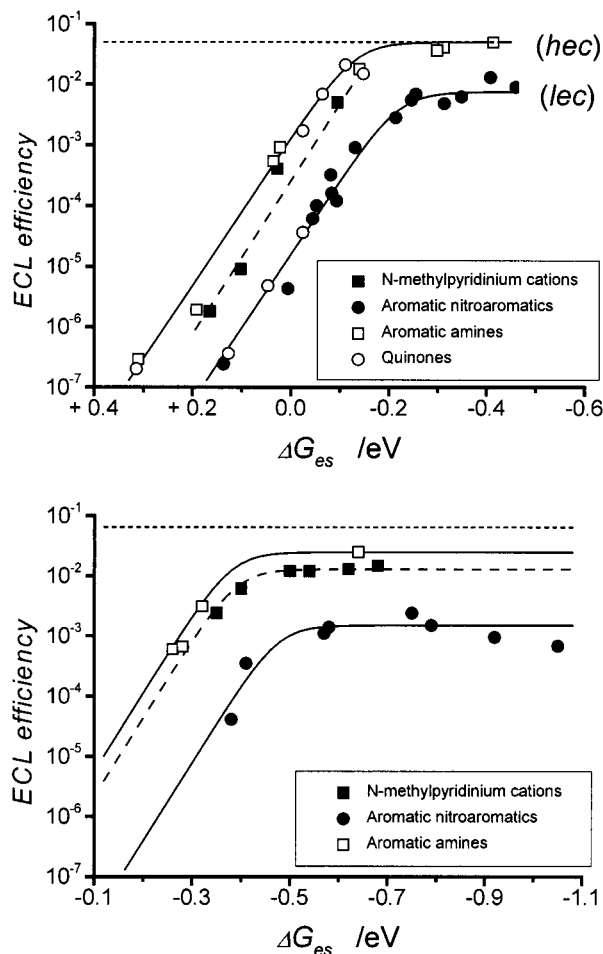


**Figure 1.** Plot of the  $\log(\phi_{\text{ecl}})$  vs  $\Delta G_{\text{es}}$  for the ECL systems involved  $\text{Ru}(\text{bipy})_3^{2+}$  (top) and  $\text{Mo}_6\text{Cl}_{14}^{2-}$  (bottom) ions in acetonitrile solutions (data from refs 19 and 20, respectively). The dotted horizontal lines correspond to the emission quantum yield of the excited  $*\text{Ru}(\text{bipy})_3^{2+}$  and  $*\text{Mo}_6\text{Cl}_{14}^{2-}$ , respectively. Other lines are drawn for ease of visualization and do not represent any theoretical fits.

tively to the population of the excited state (low exergonic reactions 1a–4a with a reaction rate  $k_{\text{es}}$ ) or to the ground state (high exergonic reactions 1b–4b with reaction rate  $k_{\text{gs}}$ ). Consequently, experimentally obtained excited-state formation efficiencies  $\phi_{\text{es}} = \phi_{\text{ecl}}/\phi_0 = k_{\text{es}}/(k_{\text{es}} + k_{\text{gs}})$  may be simply predicted if the appropriate rate constants are available from other experimental data and/or theoretical considerations. In our previous work, we applied the former approach. It is possible in view of the expected relationship between ET generation and reductive or oxidative ET quenching of the excited  $*\text{RuL}_3^{2+}$  (vide infra). ET quenching scheme<sup>22–27</sup> includes back-ET to give the ground state and a competitive step where redox products separate in solutions. For the given quencher, all the rate constants can be determined by means of the kinetic data from the luminescence quenching and transient absorption measurements. The kinetic parameters derived from the literature data (unfortunately available only for some of the systems studied) have allowed for a quantitative description of the ECL efficiency for some of the ECL systems investigated. For other ECL systems, however, the discrepancies between the experimentally found ECL efficiencies and those predicted from the quenching data were as large as a few orders of magnitude. The finding that the plot of the quenching rate constants  $k_{\text{q}}$  versus  $\Delta G_{\text{q}}$  (where  $\Delta G_{\text{q}} = -\Delta G_{\text{es}}$ ) is quite uniform for all quenchers (cf. Figure 5) allowed us<sup>19</sup> to propose that an

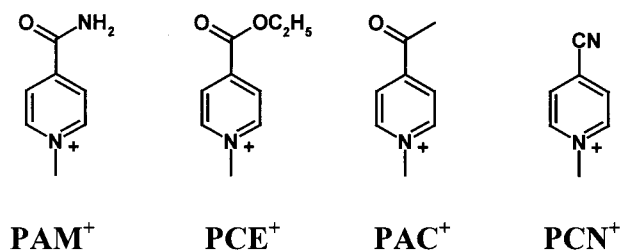


**Figure 2.** Formulas of *N*-methylpyridinium cations studied and their abbreviations used in the text.

additional, unknown factor(s) contribute(s) to the overall ECL mechanism.

As mentioned above, literature data concerning ET quenching of the excited  $^*RuL_3^{2+}$  (especially results from the transient absorption studies) are incomplete, especially in organic solvents such as ACN. For example, to our best knowledge, ET quenching of  $^*RuL_3^{2+}$  in reaction with *N*-methylpyridinium cations has been studied only in aqueous solutions.<sup>28,29</sup> Therefore, in our preliminary investigations, we were not able to compare kinetic scheme for the ECL and ET quenching processes for all of the investigated systems and, consequently, discuss a possible reason(s) of observed inconsistencies in more details. Thus, we have decided to start complementary (photo-physical) investigations. Here, we report the results of the comparative studies of the excited  $^*RuL_3^{2+}$  generation (ECL) and annihilation (oxidative quenching) in the ET reactions involving *N*-methylpyridinium radicals or *N*-methylpyridinium cations, respectively.

## 2. Experimental Section

**2.1. Materials.** Tris(2,2'-bipyridine)ruthenium(II) and tris(1,10-phenanthroline)ruthenium(II) perchlorates were synthesized using procedure described in the literature<sup>30,31</sup> and purified by means of re-crystallization from acetonitrile/toluene mixtures.

The hexafluorophosphate salts of the studied *N*-methylpyridinium cations (Figure 2) were obtained by the addition of an excess of KPF<sub>6</sub> to aqueous solution of the corresponding iodides (synthesized by addition of CH<sub>3</sub>I to an acetone solution of the appropriately substituted pyridine), following by recrystallization of the precipitated products from water.

Tetraethylammonium hexafluorophosphate was prepared by metathesis of aqueous tetraethylammonium bromide (C<sub>2</sub>H<sub>5</sub>)<sub>4</sub>NBr with KPF<sub>6</sub> solutions. The precipitated product was washed with water and re-crystallized from anhydrous methanol. Before use, the supporting electrolyte was dried in a vacuum (at 100 °C) for 12h.

Acetonitrile (ACN) was dried and purified for electrochemical use in a conventional manner. The solutions studied, containing 0.1 M (C<sub>2</sub>H<sub>5</sub>)<sub>4</sub>NPF<sub>6</sub> as the supporting electrolyte, ruthenium complex Ru(bipy)<sub>3</sub><sup>2+</sup> or Ru(phen)<sub>3</sub><sup>2+</sup>, and *N*-methylpyridinium hexafluorophosphates as the organic reaction partner, were deaerated with pure argon. All, electrochemical and spectroscopic measurements have been performed at room temperature 25 °C.

**2.2. Electrochemical and Electrochemiluminescence Instrumentation.** The same electrochemical cell was used for the electrochemical and ECL studies.<sup>32</sup> The working electrode (polished before each use with diamond paste) was a Pt disk with a diameter of 1 mm. The counter electrode was a Pt ring with inner and outer diameters of 4 and 8 mm, respectively. The separation distance between the electrodes was about 2 mm. Tungsten wire dipped in the solutions was used as the quasi-

reference electrode with a potential stable within the time scale of the experiment (ca. -0.1 V vs aqueous saturated calomel electrode). Additionally measured potentials were referred to ferrocene/ferricenium internal reference redox couple. A quartz optical fiber (with a diameter of 4 mm) passed through the counter electrode was used to collect the light emitted at the working electrode. The lateral fiber face was protected to minimize the light losses, and only the front face of the fiber was immersed directly in the solution. The end fiber face was interfaced to the photon detection system through the grating CVI Digikröm CM110 monochromator. The dispersed emission was detected using a 9816QA photomultiplier (cooled to -30 °C in FACT 50 MK III housing) with signal passed to a C10 photon counter (all parts from Thorn-EMI). The spectral response of the light detection system was calibrated with a tungsten lamp as the standard of spectral irradiance. The sensitivity threshold of the photon detection part of our equipment was about 10<sup>-7</sup>. The "electrochemical" part of the measuring system was constructed from an ELPAN EP22 potentiostat equipped with a Hameg HM205-2 digital storage scope that recorded the current and potential transients. A Pentium PC computer equipped with an Ambex AD, DA, and DD cards have been used to control the wavelength of the monochromator as well as the inputs/outputs from the potentiostat or the photon counter.

**2.3. Electrochemical and Electrochemiluminescence Measurements.** Cyclic voltammetry was run prior to the ECL measurements (to evaluate the electrochemical characteristics) as well as after ECL experiments (to check the temporal stability of the system studied). Application of a triple-step potential technique<sup>1-5</sup> causes an emission (identical with that observed in photoexcitation) to appear. The experiment began with the working electrode at a potential of no electroactivity. The potential limits of the programmed sequence were chosen to ensure production of the electrogenerated intermediates in the mass-transfer-controlled region and to minimize the influence of secondary electrochemical reactions. Subsequently, the electrode potential was again changed to the initial value. In all the cases, ECL emissions were observed during the second reactant generation step in the course of a triple-potential-step sequence. The system was allowed to equilibrate for a few seconds between each pulse sequence. The ECL spectra obtained were integrated to obtain the total photon intensities. The values of the measured integrated photon intensities were the averages of several independent measurements. For a particular solution, two or three records were made to check the temporal stability of the system studied. ECL yields were determined against the standard (ECL system containing 1mM of Ru(bipy)<sub>3</sub><sup>2+</sup> in 0.1M (C<sub>2</sub>H<sub>5</sub>)<sub>4</sub>NPF<sub>6</sub>/ACN with  $\phi_{ecl} = 0.05$ ) by comparison of the measured integrated photon intensities, taking into account also the differences in the electric charges passed through the solution studied. The error of  $\phi_{ecl}$  determination was estimated to be 10-15%.

**2.4. Spectroscopic Instrumentation.** UV-vis absorption spectra were recorded using Shimadzu UV2401 or UV3100 spectrometers, luminescence spectra by means of a "Jasny multifunctional spectrofluorimeter".<sup>33</sup> Transient absorption measurements were done using a home-built setup. The laser system used as excitation source was a pulsed Coumarine47 FL105 dye laser (emission at 456 nm with ca. 18% energy conversion) pumped by a Compex120 XeCl-excimer laser (emission at 308 nm with 100 mJ pulse energy, 10 Hz repetition rate, and 10 ns pulse width). Both lasers purchased from Lambda Physics. Typically 2-3 mJ energies (at laser beam diameter ca. 0.5 cm)

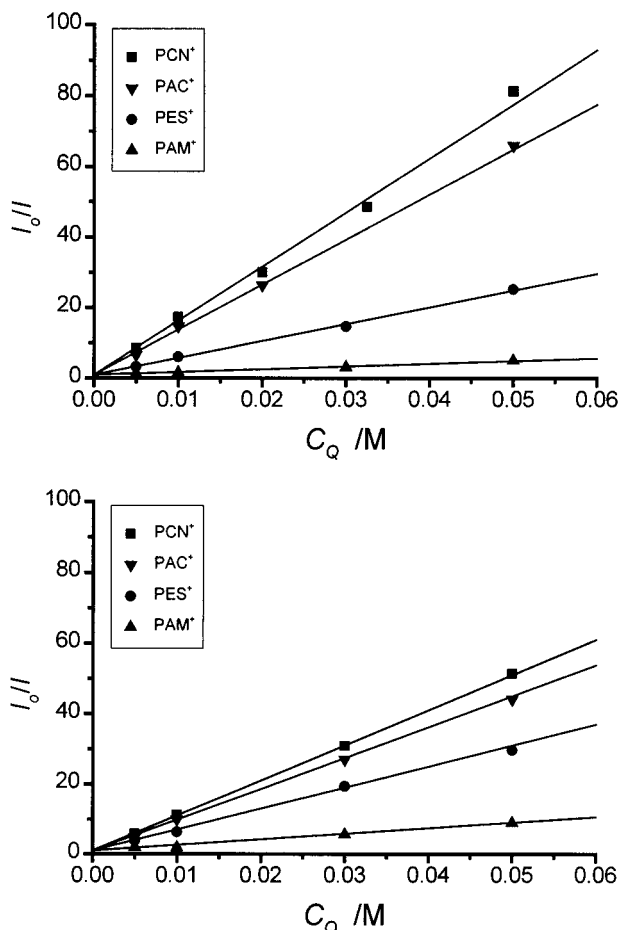


**Figure 3.** Stern–Volmer plots of the  $I_0/I$  ratio vs quencher concentration  $C_Q$  in the ET quenching of  $^*Ru(bipy)_3^{2+}$  (top) and  $^*Ru(phen)_3^{2+}$  (bottom) ions in acetonitrile solutions.

were passed into the studied solutions in the  $1 \times 1 \text{ cm}^2$  flow-through cell (with flow rates of ca.  $5 \text{ cm}^3/\text{min}$ ). For the transient detection, the light of a continuous 150W Xe-lamp was focused perpendicularly to the excitation. Detection was made by a PTI OBB101/102 monochromator fixed at the proper wavelength. The signals were detected by a Hamamatsu R928P photomultiplier connected to a Lecroy 9350C digital scope.

**2.5. Photophysical Measurements.** Samples for quenching measurements in ACN solutions contained  $1\text{--}3 \times 10^{-5} \text{ M}$  of Ru(II) complex with the appropriate concentration of added quencher. In typical experiments, emission measurements have been performed for solutions containing a few different concentrations of quencher  $C_Q$ .  $Ru(bipy)_3^{2+}$  or  $Ru(phen)_3^{2+}$  solutions (containing  $0.1 \text{ M}$   $(C_2H_5)_4NPF_6$ ) without added quencher served as a standard for the  $I_0$  emission intensity determination, respectively. Quenching rate constants  $k_q$  were determined by the steady-state Stern–Volmer method

$$\frac{I_0}{I} = 1 + k_q \tau_L C_Q \quad (6)$$

where  $I_0$ ,  $I$ , and  $\tau_L$  are the emission intensities in the absence or presence of quencher and emission lifetime of the given  $^*RuL_3^{2+}$  emitter, respectively. In all the cases, plots of  $I_0/I$  versus  $C_Q$  were linear with an intercept close to unity (cf. Figure 3). Literature values<sup>34,35</sup> of  $\tau_L = 0.85 \mu\text{s}$  for  $^*Ru(bipy)_3^{2+}$  and  $0.40 \mu\text{s}$  for  $^*Ru(phen)_3^{2+}$  in ACN solutions have been applied for  $k_q$  estimations, correspondingly. Estimated error in the determination of  $k_q$  values was found to be smaller than 10–15%.

Transient absorption measurements of the redox product separation efficiencies ( $\phi_{\text{sep}}$ ) have been performed in usual way by monitoring the absorbance changes following photoexcitation of  $\sim 1.5 \times 10^{-4} \text{ M}$   $RuL_3^{2+}$  solution containing an appropriate excess of the  $R^+$  quencher. It was done with assumption that photoproduction of the  $N$ -methylpyridinium radical  $R^*$  is equal to that of the oxidized form of ruthenium complex  $RuL_3^{3+}$  (cf. reaction mechanism presented in Figure 6). Consequently, transient absorption signal at the observation wavelength  $\lambda_{\text{obs}}$  is proportional to the difference  $\Delta\epsilon_M$  in molar extinction coefficients  $\epsilon_M$  of all the redox forms involved in ET process:

$$\Delta\epsilon_M = \epsilon_M(RuL_3^{3+}) + \epsilon_M(R^*) - \epsilon_M(RuL_3^{2+}) - \epsilon_M(R^+) \quad (7)$$

Taking into account available UV–vis data of all involved species, the observation wavelength ( $\lambda_{\text{obs}} = 375 \text{ nm}$  for  $Ru(bipy)_3^{2+}$  and  $363 \text{ nm}$  for  $Ru(phen)_3^{2+}$ ) was selected to maximize  $\Delta\epsilon_M$  term ( $3\text{--}4 \times 10^3 \text{ M}^{-1}\text{cm}^{-1}$  in both cases). Aqueous solution data<sup>36</sup> (well-known for  $RuL_3^{2+}$  and  $RuL_3^{3+}$  complexes with bipy or phen ligands) have been used for the calculation of the difference in  $\epsilon_M(RuL_3^{3+})$  and  $\epsilon_M(RuL_3^{2+})$  parameters. To our best knowledge (cf. also ref 37), contrary to Ru(II) complexes,<sup>35</sup> no literature data are available for both  $Ru(bipy)_3^{3+}$  and  $Ru(phen)_3^{3+}$  cations in ACN solutions. However, our preliminary thin-layer spectro-electrochemical studies allowed also us to conclude that the solvent induced changes in UV–vis absorption spectra of  $RuL_3^{2+}$  as well as of  $RuL_3^{3+}$  species are only minor. The necessary UV–vis absorption data (molar extinction coefficients and band shapes) of  $R^*$  radicals ( $R^+$  cations do not absorb at the selected observation wavelength) were taken from the literature (ref 38 for PES• and PAM• derivatives in ACN solutions and ref 28 for PAC• in  $H_2O$  solutions, respectively). In the case of PCN• radical, a molar extinction coefficient of about  $6 \times 10^4 \text{ M}^{-1} \text{ cm}^{-1}$  has been assumed in the interpretation of the transient absorption experiments because only qualitative UV–vis data<sup>39</sup> can be found in the literature. This assumption seems to be justified because UV–vis spectra for all  $R^*$  radicals (and  $R^+$  cations, correspondingly) involved in the presented study are close one to another<sup>28,38,39</sup> with similar absorption band positions (and shapes) and with similar extinction coefficient values. Absolute values of  $\phi_{\text{sep}}$  efficiencies have been estimated using tetracene<sup>40</sup> ( $\sim 5.5 \times 10^{-4} \text{ M}$  oxygen free cyclohexane solutions) as a reference system. Results from the triplet–triplet absorption decay measurements with the singlet–triplet intersystem crossing efficiency  $\phi_{\text{ST}} = 0.63$  and the molar extinction coefficient of the triplet–triplet absorption  $\epsilon_{\text{TT}} = 2.54 \times 10^4 \text{ M}^{-1} \text{ cm}^{-1}$  at  $485 \text{ nm}$  were used as parameters in the calculation procedure. Moreover, additional corrections were made for the percentage of quenching (third term in eq 8 which was always at least 85%) as well as for the differences of light amount absorbed by the studied and the reference samples (fourth term in eq 8):

$$\phi_{\text{sep}} = \phi_{\text{ST}} \frac{A_S/\Delta\epsilon_M}{A_R/\epsilon_{\text{TT}}} \frac{1 + k_q \tau_L C_Q (1 - 10^{-x_1 E_R}) 10^{-x_2 E_R}}{k_q \tau_L C_Q (1 - 10^{-x_1 E_S}) 10^{-x_2 E_S}} \quad (8)$$

where  $A_S$  or  $A_R$  are measured absorbances (values extrapolated to time  $t_{\text{meas}} = 0$  after the laser excitation, cf. Figure 4) of the sample and reference solutions with  $E_S$  and  $E_R$  extinctions, respectively;  $x_1$  and  $x_2$  are the parameters corresponding to the geometrical arrangement of the excitation and monitoring beams (cf. insertion in Figure 4). Terms  $(1 - 10^{-x_1 E})$  and  $10^{-x_2 E}$  (from the Lambert-Berr law) describe the amount of the light absorbed in the monitored region and the inner filter effect, respectively.

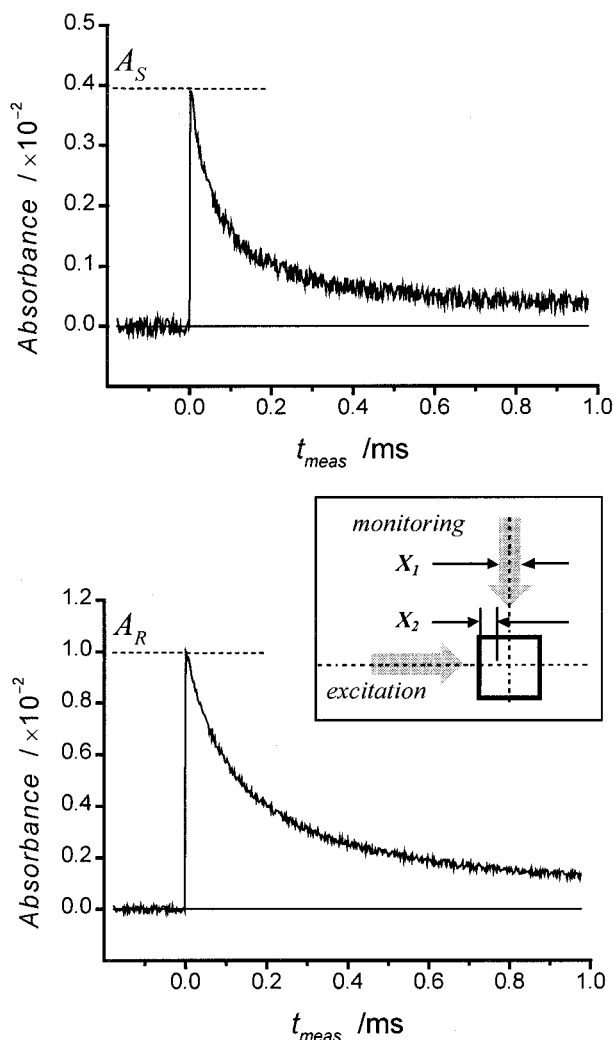


**Figure 4.** Transient absorbance decay curves recorded for sample system—Ru(bipy)<sub>3</sub><sup>2+</sup>—PCE<sup>+</sup> in acetonitrile (top) and reference—tetracene in cyclohexane (bottom) solutions. Insertion presents arrangement of the excitation and monitoring beams.

The estimated error in  $\phi_{\text{sep}}$  (caused by  $2 \times 10^{-4}$  detection limit of the measured  $A_S$  or  $A_R$  transient absorbances and all uncertainties in other terms of eq 8) was found to be ca. 15–25%.

### 3. Results and Discussion

**3.1. Quenching Rate Constants.** The rate constants  $k_q$  for the quenching of \*Ru(bipy)<sub>3</sub><sup>2+</sup> and \*Ru(phen)<sub>3</sub><sup>2+</sup> complexes (in 0.1M (C<sub>2</sub>H<sub>5</sub>)<sub>4</sub>NPF<sub>6</sub> ACN solutions) are summarized in Table 1 together with the estimated  $\Delta G_q$  values.  $\Delta G_q$  have been calculated according to eq 5 ( $\Delta G_q = -\Delta G_{\text{es}}$ ) using  $E_{\text{MLCT}} = 2.10$  eV<sup>41,42</sup> for \*Ru(bipy)<sub>3</sub><sup>2+</sup> and  $E_{\text{MLCT}} = 2.15$  eV for \*Ru(phen)<sub>3</sub><sup>2+</sup>. The latter quantity was estimated by comparison of the 77 K and room-temperature luminescence of Ru(bipy)<sub>3</sub><sup>2+</sup> and Ru(phen)<sub>3</sub><sup>2+</sup> taking into account about 0.05 eV shift<sup>35</sup> in their maxima positions. As expected, the more exergonic the electron-transfer reaction is (expressed in terms of  $\Delta G_q$  values), the faster the quenching process will be, similar to what was found previously<sup>28,29</sup> in aqueous solutions. However, the observed reaction rates are slower than in H<sub>2</sub>O. It seems to be understandable because  $\Delta G_q$  values are less negative in ACN as compared to those of water.  $k_q$  values measured in ACN solutions are at least few times slower than the diffusion limited bimolecular processes and, consequently, correspond directly

**TABLE 1: Electrochemical and Quenching Data for RuL<sub>3</sub><sup>2+</sup> + R<sup>+</sup> Systems: Redox Potentials<sup>a</sup> ( $E_{\text{ox}}$  and  $E_{\text{red}}$ ), Gibbs Energies for the Excited \*RuL<sub>3</sub><sup>2+</sup> Oxidative ET Quenching ( $\Delta G_q$ ), Experimental Values of the Quenching Rate Constants ( $k_q$ ), Estimated Values of the Forward ET Reaction ( $k_{23}$ ), and Separation Efficiencies of the ET Reaction Products ( $\phi_{\text{sep}}$ )**

complex	$E_{\text{ox}}$ /V	quencher	$E_{\text{red}}$ /V	$\Delta G_q$ /eV	$k_q$ /M <sup>-1</sup> s <sup>-1</sup>	$k_{23}$ /s <sup>-1</sup>	$\phi_{\text{sep}}$
Ru(bipy) <sub>3</sub> <sup>2+</sup>	+0.88	PAM <sup>+</sup>	-1.32	0.10	$9.1 \times 10^7$	$1.3 \times 10^8$	0.27
		PCE <sup>+</sup>	-1.19	-0.03	$5.6 \times 10^8$	$8.1 \times 10^8$	0.29
		PAC <sup>+</sup>	-1.12	-0.10	$1.5 \times 10^9$	$2.2 \times 10^9$	0.32
		PCN <sup>+</sup>	-1.05	-0.17	$1.8 \times 10^9$	$2.6 \times 10^9$	0.53
Ru(phen) <sub>3</sub> <sup>2+</sup>	+0.89	PAM <sup>+</sup>	-1.32	0.06	$4.0 \times 10^8$	$5.8 \times 10^8$	0.21
		PCE <sup>+</sup>	-1.19	-0.07	$1.5 \times 10^9$	$2.6 \times 10^9$	0.18
		PAC <sup>+</sup>	-1.12	-0.14	$2.3 \times 10^9$	$3.3 \times 10^9$	0.05
		PCN <sup>+</sup>	-1.05	-0.21	$2.5 \times 10^9$	$3.6 \times 10^9$	0.17

<sup>a</sup> Redox potentials for one-electron oxidation RuL<sub>3</sub><sup>2+</sup> + e<sup>-</sup> ⇌ RuL<sub>3</sub><sup>3+</sup> and one-electron reduction R<sup>+</sup> + e<sup>-</sup> ⇌ R• according to ferrocene/ferricenium internal reference redox couple (with  $E_{\text{ox}} = +0.41$  V vs aqueous saturated calomel electrode).

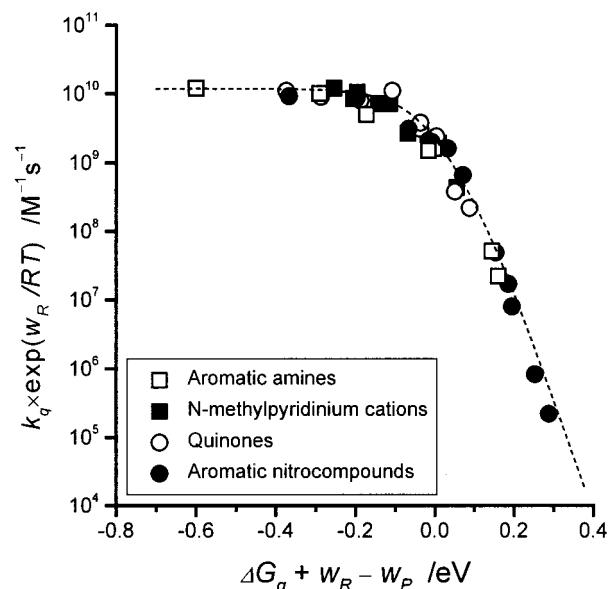


**Figure 5.** Electron-transfer quenching rate constant  $k_q$  of the excited \*RuL<sub>3</sub><sup>2+</sup> in acetonitrile solutions as a function of the reaction exergonicity  $\Delta G_q$ . The dotted line is drawn for ease of visualization and do not represent any theoretical fit.

to an activation-controlled process. The free energy relationship between  $k_q$  and  $\Delta G_q$  is shown in Figure 5, together with the data for reductive quenching of \*Ru(bipy)<sub>3</sub><sup>2+</sup> by D and oxidative quenching of \*Ru(bipy)<sub>3</sub><sup>2+</sup> by A for comparison.

The observed relationship between respectively corrected  $k_q$  and  $\Delta G_q$  is uniform and does not depend significantly on the nature of the organic reaction partner.  $k_q$  and  $\Delta G_q$  values were corrected for the differences in the Coulomb interaction energies required to bring the reactants ( $w_R$ ) or products ( $w_P$ ) together at the most probable separation distance  $d$  at which the electron transfer takes place. The necessary terms  $w_R$  and  $w_P$  were calculated according to familiar Debye equations.<sup>43,44</sup> Corresponding  $w_R$  and  $w_P$  values are rather small, e.g.,  $w_R = 0.04$  and  $w_P = 0.00$  eV have been calculated for the case of studied RuL<sub>3</sub><sup>2+</sup>—R<sup>+</sup> systems with  $d = 1.1$  nm as the sum of the effective radii<sup>23</sup> of RuL<sub>3</sub><sup>2+</sup> (0.71 nm) and R<sup>+</sup> (0.39 nm).

**3.2. Reaction Mechanism of the Oxidative Electron-Transfer Quenching.** Oxidative ET quenching of the excited \*Ru(bipy)<sub>3</sub><sup>2+</sup> and \*Ru(phen)<sub>3</sub><sup>2+</sup> by R<sup>+</sup> cations may be quantitatively discussed according to the reaction mechanism scheme<sup>45,46</sup> (presented in Figure 6) where  $k_{12}$  and  $k_{21}$  are the diffusion-

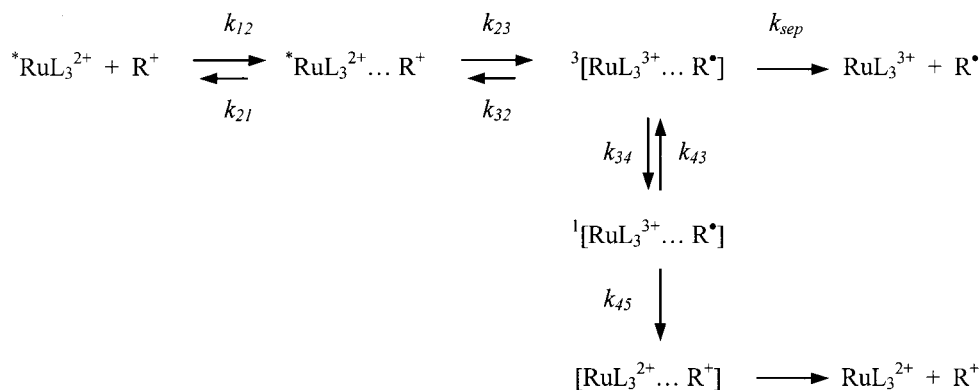


**Figure 6.** Reaction mechanism for the electron-transfer quenching of the excited  $*RuL_3^{2+}$ .

controlled forward and reverse rate constants for the formation of an activated complex (with the equilibrium constant  $K_{12} = k_{12}/k_{21}$ ) between the excited  $*RuL_3^{2+}$  and quencher  $R^+$ . The activated complex is formed from the excited triplet state of  $RuL_3^{2+}$  so that ET product appears (with the forward electron-transfer rate  $k_{23}$ ) also in the triplet state (because of the spin conservation rule). As usual, the redox products  $R^*$  and  $RuL_3^{3+}$  may be separated in solutions (with the rate  $k_{sep}$  and efficiency  $\phi_{sep}$ ) if the recombination to the singlet ground state product is sufficiently slow. The latter is allowed from the singlet precursor but forbidden from the triplet one. Therefore, the triplet–singlet conversion, occurring with rate  $k_{34}$ , is a necessary step that makes back electron transfer to the ground-state product (with rate  $k_{45}$ ) possible. The scheme includes also the reverse electron transfer corresponding to the back electron transfer to the excited state (with the rate  $k_{32}$ ) and the singlet–triplet conversion (with rate the  $k_{43}$ ). Taking into account presumably very small energy splitting between two spin forms of the primary electron-transfer product ( ${}^1[RuL_3^{3+} \cdots R^*]$  and  ${}^3[RuL_3^{3+} \cdots R^*]$ , respectively), one can conclude that  $3k_{43} = k_{34}$ . The latter process is relatively slow ( $3k_{43} \ll k_{45}$ )<sup>45,46</sup> as compared to the ground product formation and may be, at least in a first-order approximation, omitted. On the other hand, the back electron transfer to the ground-state products is extremely fast<sup>45,46</sup> ( $k_{45} \gg k_{sep}$ ) that allows to neglect a separation of  ${}^1[RuL_3^{3+} \cdots R^*]$  pair into isolated products  $RuL_3^{3+}$  and  $R^*$ .

It should be noted that in a more commonly accepted scheme<sup>22–28</sup> spin conservation rule was not taken into account. It corresponds formally to the case of infinitely fast spin dynamics and to the conclusion that the ground-state product population is governed by intrinsic electron transfer step. It is principally incorrect<sup>47</sup> and leads to wrong interpretation of the experimental data (e.g., discussion of the observed reaction rates in terms of Marcus theory with suggestions of the evidence of the inverted Marcus region).

The observed bimolecular quenching rate constant  $k_q$  is related to the rate constants of all reaction steps. If the diffusional limitation can be neglected (as it is in the present case), the kinetic scheme as discussed above may be easily solved in the steady-state approximation. Assuming above-mentioned simplifications, i.e.  $3k_{43} \ll k_{45}$  and  $k_{45} \gg k_{sep}$ , the quenching rate constant may be expressed as follows:

$$k_q = \frac{K_{12}k_{23}(k_{34} + k_{sep})}{(k_{32} + k_{34} + k_{sep})} \quad (9)$$

Equation 9 may be further simplified to  $k_q = K_{12}k_{23}$  because results from transient absorption as well as from ECL studies (vide infra) indicate that the sum  $k_{34} + k_{sep}$  is much larger, at

least 1 order of magnitude, than  $k_{32}$ . Thus,  $k_{23}$  rate constants can be simply evaluated from the experimental values of  $k_q$  using the formation constant of the activated complex  $K_{12} = 0.69M^{-1}$  as straightforwardly calculated according to the Fuoss-Eigen model:<sup>48,49</sup>

$$K_{12} = \frac{4\pi N_A d^3}{3000} \exp(-w_R/RT) \quad (10)$$

where  $N_A$ ,  $R$ , and  $T$  are the Avogadro constant, the gas constant, and absolute temperature, correspondingly. Obtained  $k_{23}$  values are presented in Table 1.

**3.3. Redox Product Separation Efficiencies.** Values of  $\phi_{sep}$  are collected in Table 1. These values (similar to those found previously in aqueous solutions<sup>29</sup>) are smaller than unity, indicating that full separation of  ${}^3[RuL_3^{3+} \cdots R^*]$  pair into  $R^*$  and  $Ru(bipy)_3^{3+}$  or  $Ru(phen)_3^{3+}$  products is not achieved.  $\phi_{sep}$  values are somewhat smaller/larger as compared to those previously reported for  $RuL_3^{2+}-D^{23,24}$  and  $RuL_3^{2+}-A^{25}$  systems, respectively. This finding may be rationalized by taking into account the Coulombic repulsive (+0.02 eV) or attractive (−0.06 eV) forces ( $w_p$ ) within  ${}^3[RuL_3^{3+} \cdots D^+]$  or  ${}^3[RuL_3^{3+} \cdots A^-]$  pairs. The Coulombic interactions cause the respective enhancement or lowering of  $k_{sep}$  rate. The effect may be estimated on the basis of the combination of Eigen's and Smoluchowski–Einstein equations:

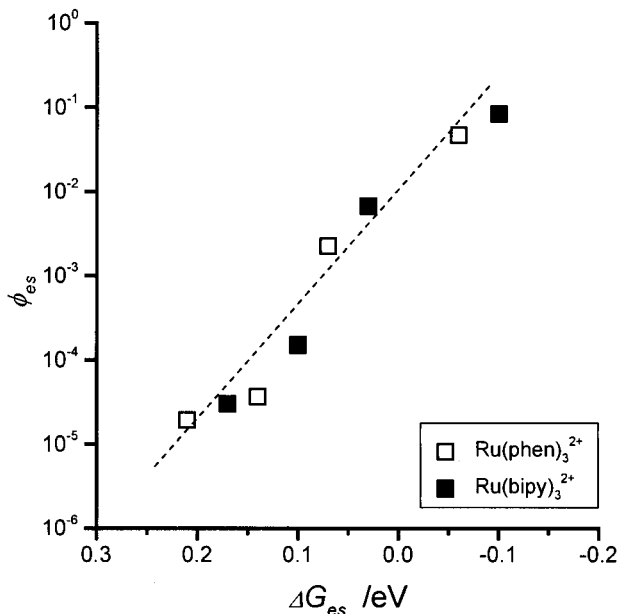
$$k_{sep} = \frac{2RT}{\pi\eta d^3 N_A} \frac{w_p/RT}{1 - \exp(-w_p/RT)} \quad (11)$$

where  $\eta$  is the medium viscosity. Appropriate calculations lead to  $k_{sep} = 6.1 \times 10^9 \text{ s}^{-1}$  for  $RuL_3^{3+} \cdots R^*$  pair. Experimental  $\phi_{sep}$  values allow for estimation of  $k_{34}$  rates. It may be done using simple relationship  $(1 - \phi_{sep})/\phi_{sep} = k_{34}/k_{sep}$ . The obtained  $k_{34}$  rates are presented in Table 2. These values (being in the range  $5.4 \times 10^9 - 1.2 \times 10^{11} \text{ s}^{-1}$ ) are comparable with previously found for  $RuL_3^{2+}-D$  or  $RuL_3^{2+}-A$  systems ( $5.9 \times 10^9 - 1.3 \times 10^{10}$  and  $2 - 3 \times 10^{10} \text{ s}^{-1}$ , respectively). One can conclude (similarly as it was already drawn in ref 50) that the triplet–singlet conversion rate  $k_{34}$  is nearly independent of the organic reactant nature.

**3.4. Electron-Transfer Generation of the Excited  $*RuL_3^{2+}$ .** The obtained ECL efficiencies (measured in 0.1M  $(C_2H_5)_4NPF_6$  ACN solutions) are collected in Table 2. As it was expected, the functional dependence of  $\phi_{ecl}$  on the electron-transfer reaction exergonicity ( $\Delta G_{es} = -\Delta G_q$ ) is observed for both  $Ru(bipy)_3^{3+}-R^*$  and  $Ru(phen)_3^{3+}-R^*$  systems.  $\phi_{ecl}$  rapidly decreases with the decrease of  $\Delta G_{es}$ . The observed relationship between  $\Delta G_{es}$  and the estimated  $\phi_{es}$  efficiencies (as calculated

**TABLE 2: Electrochemiluminescence Data for RuL<sub>3</sub><sup>3+</sup> + R<sup>•</sup> Systems: Gibbs Energies for the Excited \*RuL<sub>3</sub><sup>2+</sup> Population (ΔG<sub>es</sub>), Experimental Values of the ECL Efficiencies (φ<sub>ec1</sub>), Values of the Excited \*RuL<sub>3</sub><sup>2+</sup> (k<sub>32</sub>) and Ground-State RuL<sub>3</sub><sup>2+</sup> (k<sub>34</sub>) Population Rate Constants, and Experimental and Calculated Values of the Excited \*RuL<sub>3</sub><sup>2+</sup> Formation Efficiencies (φ<sub>es</sub>)**

complex	radical	ΔG <sub>es</sub> /eV	φ <sub>ec1</sub>	k <sub>32</sub> /s <sup>-1</sup>	k <sub>34</sub> /s <sup>-1</sup>	φ <sub>es</sub> (exp)	φ <sub>es</sub> (calc)
Ru(bipy) <sub>3</sub> <sup>3+</sup>	PAM <sup>•</sup>	-0.10	5.0 × 10 <sup>-3</sup>	1.4 × 10 <sup>9</sup>	1.7 × 10 <sup>10</sup>	8.3 × 10 <sup>-2</sup>	5.8 × 10 <sup>-2</sup>
	PCE <sup>•</sup>	0.03	4.0 × 10 <sup>-4</sup>	5.3 × 10 <sup>8</sup>	1.5 × 10 <sup>10</sup>	1.7 × 10 <sup>-3</sup>	2.6 × 10 <sup>-3</sup>
	PAC <sup>•</sup>	0.10	9.0 × 10 <sup>-6</sup>	9.2 × 10 <sup>7</sup>	1.3 × 10 <sup>10</sup>	1.5 × 10 <sup>-4</sup>	5.3 × 10 <sup>-4</sup>
	PCN <sup>•</sup>	0.17	1.8 × 10 <sup>-6</sup>	7.1 × 10 <sup>5</sup>	5.4 × 10 <sup>9</sup>	3.0 × 10 <sup>-5</sup>	9.9 × 10 <sup>-5</sup>
Ru(phen) <sub>3</sub> <sup>3+</sup>	PAM <sup>•</sup>	-0.06	1.4 × 10 <sup>-3</sup>	1.3 × 10 <sup>9</sup>	2.3 × 10 <sup>10</sup>	7.0 × 10 <sup>-2</sup>	3.9 × 10 <sup>-2</sup>
	PCE <sup>•</sup>	0.07	6.7 × 10 <sup>-5</sup>	3.6 × 10 <sup>7</sup>	2.8 × 10 <sup>10</sup>	3.4 × 10 <sup>-3</sup>	1.0 × 10 <sup>-3</sup>
	PAC <sup>•</sup>	0.14	1.1 × 10 <sup>-6</sup>	2.9 × 10 <sup>6</sup>	1.2 × 10 <sup>11</sup>	5.5 × 10 <sup>-5</sup>	1.9 × 10 <sup>-5</sup>
	PCN <sup>•</sup>	0.21	5.8 × 10 <sup>-7</sup>	2.1 × 10 <sup>5</sup>	3.0 × 10 <sup>10</sup>	2.9 × 10 <sup>-5</sup>	0.5 × 10 <sup>-5</sup>

**Figure 7.** Plot of the log(φ<sub>es</sub>) vs ΔG<sub>es</sub> for the ECL systems involved Ru(bipy)<sub>3</sub><sup>2+</sup> and Ru(phen)<sub>3</sub><sup>2+</sup> ions in acetonitrile solutions. The dotted line is drawn for ease of visualization and do not represent any theoretical fits.

using the quantum yield φ<sub>o</sub> = 0.06<sup>51</sup> for \*Ru(bipy)<sub>3</sub><sup>2+</sup> and 0.02<sup>35</sup> for \*Ru(phen)<sub>3</sub><sup>2+</sup> is quite uniform for both ruthenium complexes studied (cf. Figure 7).

The corresponding scheme (Figure 8) illustrating the generation of excited \*RuL<sub>3</sub><sup>2+</sup> in an electrochemiluminescence (ECL) experiment should be essentially the reverse to that postulated for the quenching reactions. The electrochemically generated, oxidized RuL<sub>3</sub><sup>3+</sup> and reduced R<sup>•</sup> species form an activated complex in two different spin states with branching ratio 3:1 (according to the spin statistic rule<sup>52,53</sup>). Electron transfer within activated complex in the triplet state <sup>3</sup>[RuL<sub>3</sub><sup>3+</sup>...R<sup>•</sup>] leads directly to the excited \*RuL<sub>3</sub><sup>2+</sup> generation. On the other hand, triplet-singlet conversion is necessary before the electron transfer to the ground-state product occurs. Activated complex <sup>1</sup>[RuL<sub>3</sub><sup>3+</sup>...R<sup>•</sup>] in the singlet state exhibits exactly opposite behavior. Electron transfer leads directly to the ground-state products, and the excited \*RuL<sub>3</sub><sup>2+</sup> formation is preceded by

singlet-triplet conversion. Taking into account the expected values of the respective processes, one can expect that the generation of \*RuL<sub>3</sub><sup>2+</sup> from <sup>3</sup>[RuL<sub>3</sub><sup>3+</sup>...R<sup>•</sup>] precursor is much more efficient with respect to the <sup>1</sup>[RuL<sub>3</sub><sup>3+</sup>...R<sup>•</sup>] one.

Kinetic scheme for the electron-transfer generation of the excited \*RuL<sub>3</sub><sup>2+</sup> can be solved (similarly as in the case of the quenching process) using steady-state approximation. In the simplified case (i.e. neglecting any diffusional limitation), one can simply obtain

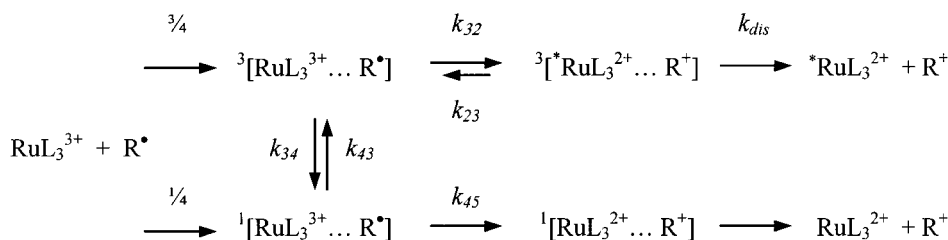
$$\frac{\phi_{es}}{1 - \phi_{es}} = \frac{3k_{32}}{4k_{34} + k_{32}} + \frac{3k_{32}}{k_{45}} \frac{4k_{34}}{4k_{34} + k_{32}} \quad (12)$$

where the first and second terms on right side correspond to the direct formation of \*RuL<sub>3</sub><sup>2+</sup> from <sup>3</sup>[RuL<sub>3</sub><sup>3+</sup>...R<sup>•</sup>] and the indirect one from <sup>1</sup>[RuL<sub>3</sub><sup>3+</sup>...R<sup>•</sup>], respectively.

Equation 12 (derived under assumption that 3k<sub>43</sub> = k<sub>34</sub>) allows simple prediction of the φ<sub>es</sub> efficiencies in view of the kinetic data from quenching and transient absorption studies. As it was mentioned above, only direct formation of \*RuL<sub>3</sub><sup>2+</sup> from <sup>3</sup>[RuL<sub>3</sub><sup>3+</sup>...R<sup>•</sup>] is an efficient process. Taking into account the possible values of k<sub>32</sub>, k<sub>34</sub>, and k<sub>45</sub> rate constants, it is expected that the contribution from the <sup>1</sup>[RuL<sub>3</sub><sup>3+</sup>...R<sup>•</sup>] precursor is much less important. Thus, the second term in eq 12 may be at least in first approximation neglected. The results of the appropriate calculations are presented in Table 2. It was done using the k<sub>34</sub> values obtained from our transient absorption studies and the k<sub>32</sub> values as estimated from the relation between k<sub>23</sub> and k<sub>32</sub>:

$$k_{32}/k_{23} = \exp[-(\Delta G_{es} + w_R - W_p)/RT] \quad (13)$$

The experimental and computed φ<sub>es</sub> values are compared in Table 2. The agreement between the two sets can be regarded as satisfactory. Similar agreement between φ<sub>es</sub>(exp) and φ<sub>es</sub>(calc) can be also obtained for other ECL systems involving Ru(bipy)<sub>3</sub><sup>2+</sup> complex. For example, using the literature data<sup>25</sup> for k<sub>32</sub> and k<sub>34</sub> rates, one can obtain φ<sub>es</sub> values of 0.06 (for 1-chloro-9,10-anthraquinone) and 0.09 (for 2-methyl-9,10-anthraquinone). These values are in a good agreement with the experimentally found 0.12 and 0.25, respectively.<sup>19</sup> Similar agreement can be also found for the ECL systems involving some aromatic amines (cf. ref 19). It allows us to conclude that most probably all of the RuL<sub>3</sub><sup>2+</sup> ECL systems assigned to the

**Figure 8.** Reaction mechanism for the excited \*RuL<sub>3</sub><sup>2+</sup> generation in the ions annihilation processes.

line (hec) in Figure 1 may be quantitatively interpreted in terms of a simple model as described above. Scatter of the experimental points around the line hec is caused by small differences in the  $k_{34}$  rates.

#### 4. Conclusions

The obtained results indicate that the intuitive relationship between ECL and electron transfer quenching mechanisms is principally correct and offers a useful approach in the explanation of the results from the ECL studies of for  $\text{Ru}(\text{bipy})_3^{2+} - \text{R}^+$  and  $\text{Ru}(\text{phen})_3^{2+} - \text{R}^+$  systems, similar to what was previously reported<sup>19</sup> for aromatic amines or anthraquinones. The kinetic data resulting from the luminescence quenching and the transient absorption experiments allow the quantitative predictions of the ECL efficiency. It may be expected that the discussed relationship (most probable from a kinetic point of view) should be also applicable in the case of the ECL systems of the lec type. Extremely fast triplet-singlet conversion between  $^3[\text{RuL}_3^{3+} \cdots \text{A}^-]$  and  $^1[\text{RuL}_3^{3+} \cdots \text{A}^-]$  forms in the cases of aromatic nitrocompounds and small quinones may be responsible for the observed relatively low (with respect to that for the ECL systems of the hec type) ECL efficiencies. Unfortunately, the lack of the necessary transient absorption data does not allow quantitative discussion of this option.

**Acknowledgment.** The Grant 3T09A06214 from the Committee of Scientific Research sponsored this work. P.S. wishes to thank the Austrian Academic Exchange Service (ÖAAD) for the financial support to visit the Technical University of Graz (exchange program no. 4/2000). Technical assistance of Mrs. B. Osińska is highly appreciated.

#### References and Notes

- (1) Faulkner, L. R.; Bard, A. J. *Electroanal. Chem.* **1977**, *10*, 1.
- (2) Park, S.-M.; Tryk, D. A. *Rev. Chem. Intermed.* **1981**, *4*, 43.
- (3) Bykh, A. I.; Vasil'ev, R. F.; Rozickij, N. N. *Itogi Nauki Tekh. Elektrokhim.* **1979**, *2*, 3.
- (4) Velasco, J. G. *Electroanalysis* **1991**, *3*, 261.
- (5) Kapturkiewicz, A. In *Advances in Electrochemical Sciences and Engineering*; Alkire, R., Gerischer, H., Kolb, D. M., Tobias, C. W., Eds.; Wiley-VCH: Weinheim, 1997; Vol. 5, p 1.
- (6) Vogler, A.; Kunkely, H.; Schäffl, S. *ACS Symp. Ser.* **1986**, *307*, 120.
- (7) Vogler, A.; Kunkely, H. *ACS Symp. Ser.* **1987**, *333*, 155.
- (8) Tokel, N. E.; Bard, A. J. *J. Am. Chem. Soc.* **1972**, *94*, 2862.
- (9) Rubinstein, I.; Bard, A. J. *J. Am. Chem. Soc.* **1981**, *103*, 6641.
- (10) Itoh, K.; Honda, K. *Chem. Lett.* **1979**, 99.
- (11) Luttmer, J. D.; Bard, A. J. *J. Phys. Chem.* **1981**, *85*, 1155.
- (12) Glass, R. S.; Faulkner, L. R. *J. Phys. Chem.* **1981**, *85*, 1160.
- (13) Wallace, W. L.; Bard, A. J. *J. Phys. Chem.* **1979**, *83*, 1350.
- (14) Bolletta, F.; Vitale, M. *Inorg. Chim. Acta* **1990**, *175*, 127.
- (15) Bolletta, F.; Bonafede, S. *Pure Appl. Chem.* **1986**, *58*, 1229.
- (16) McCord, P.; Bard, A. J. *J. Electroanal. Chem.* **1991**, *318*, 91.
- (17) Velasco, J. G. *J. Phys. Chem.* **1988**, *92*, 2202.
- (18) Kapturkiewicz, A. *Chem. Phys. Lett.* **1995**, *236*, 389.
- (19) Szrebowsky, P.; Kapturkiewicz, A. *Chem. Phys. Lett.* **2000**, *328*, 160.
- (20) Mussel, R. D.; Nocera, D. G. *J. Am. Chem. Soc.* **1988**, *110*, 2764.
- (21) Marcus, R. A. *J. Chem. Phys.* **1965**, *43*, 2654.
- (22) Bock, C. R.; Connor, A. R.; Gutierrez, A. R.; Meyer, T. J.; Whitten, D. G.; Sullivan, B. P.; Nagle, J. K. *J. Am. Chem. Soc.* **1979**, *101*, 4815.
- (23) Kitamura, N.; Kim, H.-B.; Okano, S.; Tazuke, S. *J. Phys. Chem.* **1989**, *93*, 5750.
- (24) Kim, H.-B.; Kitamura, N.; Kawanishi, Y.; Tazuke, S. *J. Phys. Chem.* **1989**, *93*, 5757.
- (25) Frank, R.; Greiner, G.; Rau, H. *Phys. Chem. Chem. Phys.* **1999**, *1*, 3481.
- (26) Ohno, T.; Yoshimura, A.; Mataga, N. *J. Phys. Chem.* **1990**, *94*, 4871.
- (27) Clark, C. D.; Hoffman, M. Z. *J. Phys. Chem.* **1996**, *100*, 14688.
- (28) Miyashita, T.; Murakata, T.; Yamaguchi, Y.; Matsuda, M. *J. Phys. Chem.* **1985**, *89*, 497.
- (29) Jones, G., II; Malba, V. *J. Org. Chem.* **1985**, *26*, 5776.
- (30) Cook, M. J.; Lewis, A. P.; McAuliffe, G. S. G.; Skarda, V.; Thomson, A. J. *J. Chem. Soc., Perkin Trans.* **1984**, 1293.
- (31) Alford, P. C.; Cook, M. J.; Lewis, A. P.; McAuliffe, G. S. G.; Skarda, V.; Thomson, A. J. *J. Chem. Soc., Perkin Trans.* **1985**, 705.
- (32) Kapturkiewicz, A. *J. Electroanal. Chem.* **1993**, *348*, 283.
- (33) Jasny, J. *J. Lumin.* **1978**, *17*, 143.
- (34) Caspar, J. V.; Meyer, T. J. *J. Am. Chem. Soc.* **1983**, *105*, 5583.
- (35) Kawanishi, Y.; Kitamura, N.; Tazuke, S. *Inorg. Chem.* **1989**, *28*, 2968.
- (36) Seddon, E. A.; Seddon, K. R. *The Chemistry of Ruthenium*; Elsevier: Amsterdam, 1984.
- (37) Juris, A.; Balzani, V.; Barigelletti, F.; Campagna, S.; Besler, P.; von Zalewsky, A. *Coord. Chem. Rev.* **1988**, *84*, 85.
- (38) Hermolin, J.; Levin, M.; Kosower, E. M. *J. Am. Chem. Soc.* **1981**, *103*, 4808.
- (39) Itoh, M.; Nagakura, S. *Bull. Chem. Soc. Jpn.* **1966**, *39*, 369.
- (40) Jardon, P.; Gautron, R. *J. chim. phys.* **1985**, *82*, 353.
- (41) Kalyanasundaram, K. *Coord. Chem. Rev.* **1983**, *46*, 159.
- (42) Sutin, N. *Acc. Chem. Res.* **1982**, *15*, 275.
- (43) Friedman, H. L. *Pure App. Chem.* **1981**, *53*, 1277.
- (44) Jensen, T. J.; Gray, H. B.; Winkler, J. R.; Kuznetsov, A. M.; Ulstrup, J. *J. Phys. Chem. B* **2000**, *104*, 11556.
- (45) Wolf, H.-J.; Bürssner, D.; Steiner, U. *Pure Appl. Chem.* **1995**, *67*, 167.
- (46) Bürssner, D.; Wolf, H.-J.; Steiner, U. *Angew. Chem., Int. Ed. Engl.* **1994**, *33*, 1772.
- (47) Burshtein, A. I. *Adv. Chem. Phys.* **2000**, *114*, 419.
- (48) Fuoss, R. M. *J. Am. Chem. Soc.* **1958**, *80*, 5059.
- (49) Eigen, M. *Z. Phys. Chem. NF.* **1954**, *1*, 176.
- (50) Shioyama, H.; Masuhara, H.; Mataga, N. *Chem. Phys. Lett.* **1982**, *88*, 161.
- (51) Caspar, J. V.; Meyer, T. J. *J. Am. Chem. Soc.* **1983**, *105*, 5583.
- (52) Saltiel, J.; Atwater, B. W. *Adv. Photochem.* **1988**, *4*, 1.
- (53) Hoytink, G. J. *Discuss. Faraday Soc.* **1968**, *5*, 14.